

# Light Metals 2014

**ALUMINUM PROCESSING**

**Extrusion & Miscellaneous  
Processes**

## A NUMERICAL AND EXPERIMENTAL STUDY OF HOMOGENIZATION OF Al-Si-Mg ALLOYS

Pikee Priya, Matthew J. M. Krane, David R. Johnson

School of Materials Engineering, Neil Armstrong Hall of Engineering, 701 Northwestern Avenue, Purdue University, West Lafayette, IN 47907, USA

Keywords: homogenization, dissolution kinetics, cooling rate

### Abstract

Homogenization is important for alloys to obtain a good surface finish, low flow stress and minimized recrystallization during extrusion. A numerical and experimental study of the homogenization process for Al-Si-Mg alloy was done. A finite volume diffusion model, coupled with a cellular automaton to predict phase change, was developed to study the dissolution kinetics for the as-cast microstructure for ternary systems. The required thermodynamic and kinetic data was provided to the model from ThermoCalc and DICTRA. Homogenization at 4 different temperatures was simulated. The volume fraction of the precipitates decreases exponentially with time. The length scales of the precipitates predicted matched the experimental length scales. The effect of cooling rate after homogenization on the precipitation behavior of the Mg<sub>2</sub>Si phase was also studied using a finite difference model. The volume fraction and mean radius of the Mg<sub>2</sub>Si particles is found to decrease with increasing cooling rate while the average Mg concentration of the matrix increases with increasing cooling rate, in accordance with the hardness results reported in [15].

### Introduction

Al-Si-Mg alloys (6xxx series) form a very important group of aluminum alloys used often for extrusions. Homogenization of Al-Si-Mg alloys is an important process step which (i) reduces microsegregation; (ii) dissolves non-equilibrium eutectic phases formed during casting; (iii) helps in spheroidization of non-soluble phases present; and (iv) facilitates precipitation of dispersoids (for alloys containing Mn and Cr). The Mg<sub>2</sub>Si phase precipitates when cooling from the homogenization temperature. Control of all these processes are essential for good surface finish; low flow stress and reduced recrystallization during hot-working.

Although there have been a number of experimental studies on homogenization and its effect on extrusion for the 6xxx series alloys [1-3], numerical studies have been comparatively fewer in number. Many numerical studies [4-7] consider 1D models to simulate homogenization. References [4,5] did not consider the cross diffusion effects in their model. References [6,7] used DICTRA to simulate removal of microsegregation and transformation of iron-containing intermetallics during homogenization. The aim here is to develop a 2D Cellular Automaton-Finite Volume model to simulate various microstructural changes occurring during homogenization and to use a 1D Finite Difference model used by Myer and Grong et al. [8] to study the effect of cooling rates after homogenization for a ternary Al-Si-Mg alloy. The numerical results are compared with the experimental study.

### Numerical Model

#### Model Description

A 2D homogenization model has been developed which is able to predict diffusion-based dissolution and growth of phases depending on temperature and curvature of the precipitate for binary and ternary systems. Software for thermodynamic calculations (Thermo-Calc) and simulation of diffusion induced phase transformations (DICTRA) were used for thermodynamic (equilibrium concentrations at different temperatures) and kinetic (diffusion coefficients) data respectively. An aluminum based mobility database is used for the calculation of diffusion coefficients. A Cellular Automaton- Finite Volume based algorithm, similar to one which has been used for liquid-solid phase transformation [9-10], is used to simulate solid-solid phase transformation at the interface.

The domain is divided into finite cells each of which is  $\alpha$ (matrix) phase,  $\beta$ (precipitate) phase or interface. An interface cell has a fraction of phase  $\beta$  between 0 and 1, the remainder volume being  $\alpha$ . The change in fraction of the precipitate phase is calculated keeping both the phases in equilibrium and conserving mass in and around the interface cell. Change in phase  $\beta$  in the interface cell conserving component A in a ternary system is given by,

$$\Delta f_p^A = \frac{(1-f_p)(C_\alpha^A - C_\alpha^{A*}) - f_p(C_\beta^A - C_\beta^{A*}) + \sum_{i=1}^n (C_i^A - C_\alpha^{A*}) + \sum_{i=1}^n (C_i^A - C_\beta^{A*})}{(C_\beta^{A*} - C_\alpha^{A*})}, \quad (1)$$

Where,  $\Delta f_p^A$  is the change in fraction of the precipitate phase calculated;  $C_\alpha^{A*}$  is the equilibrium concentration of the matrix phase;  $C_\beta^{A*}$  is the equilibrium concentration of the precipitate phase;  $C_\alpha^A$  is the concentration of the matrix phase of the cell;  $C_\beta^A$  is the concentration of the precipitate phase of the cell;  $C_i^A$  is the concentration of the matrix or precipitate phase of the neighboring cells all for component A and  $f_p$  is the fraction of the precipitate phase in the cell.

$$\Delta f_p^B = \frac{(1-f_p)(C_\alpha^B - C_\alpha^{B*}) - f_p(C_\beta^B - C_\beta^{B*}) + \sum_{i=1}^n (C_i^B - C_\alpha^{B*}) + \sum_{i=1}^n (C_i^B - C_\beta^{B*})}{(C_\beta^{B*} - C_\alpha^{B*})} \quad (2)$$

For equilibrium to be maintained in both the phases,

$$\Delta f_p^A = \Delta f_p^B \quad (3)$$

Phase  $\beta$  grows or dissolves depending on the sign of  $\Delta f_p$ . The curvature of the interface is calculated using the height function method [11]. The Thompson-Freundlich equation [12] is used to calculate the equilibrium concentration of matrix phase due to curvature assuming concentration change for the precipitate phase due to curvature is negligible. In the process of growth or dissolution, the amount of solute absorbed or rejected by the interface cell is taken from or distributed among the neighboring cells such that both the phases attain equilibrium.

This growth algorithm is coupled with finite volume solution of Fick's second law of diffusion equation:

$$\frac{dC_A}{dt} = D_{AA}^C \left[ \frac{d^2C_A}{dx^2} + \frac{d^2C_A}{dy^2} \right] + D_{AB}^C \left[ \frac{d^2C_B}{dx^2} + \frac{d^2C_B}{dy^2} \right], \quad (4)$$

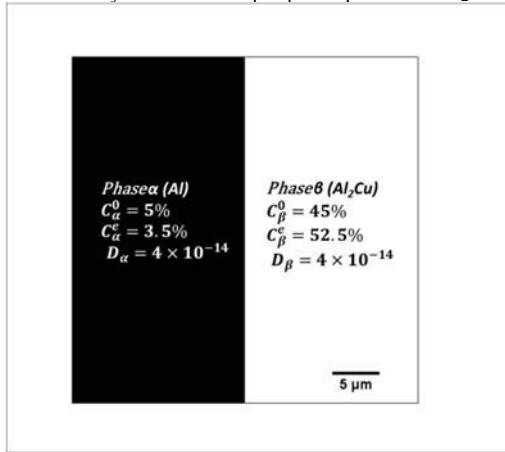
Where effect of one species on the diffusion of the other is taken into account by including the cross diffusion coefficients,  $D_{AB}^C$ . Here, Gauss-Siedel with successive over relaxation and an implicit scheme of time integration are used to solve the discretized equations.

An initial as-cast microstructure with 10% volume fraction of the eutectic consisting of 15%  $Mg_2Si$  as given by the pseudo-binary phase diagram of  $Mg_2Si$  and Al [13] is considered. The concentration profiles assuming a Scheil-type solidification is considered.

To study the effect of cooling rate on precipitation of the  $Mg_2Si$  phase, a finite difference based model used by Myer and Grong et. al. [8] is used.

### Model Validation

The 1D binary homogenization model has been validated against the analytical solution [17]. A 2 phase Al- $Al_2Cu$

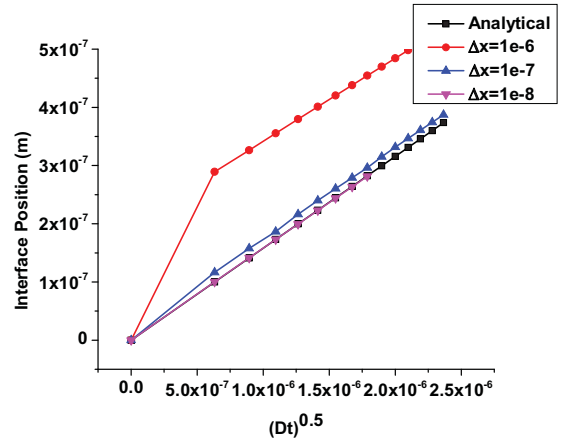


(a)

diffusion couple is chosen for the validation, where the position of the interface changes due to difference in equilibrium concentrations of both the phases. The initial and final concentrations of the two phases and the diffusion coefficient chosen for the validation test are shown in Figure 1(a). A grid dependence study has also been done. (Figure 1(b)). The solutions are found to closely match the analytical solution for grid size of  $1 \times 10^{-8}$  m. Also, the binary and ternary models have been validated with well-known transformations from DICTRA, such as austenite to ferrite.

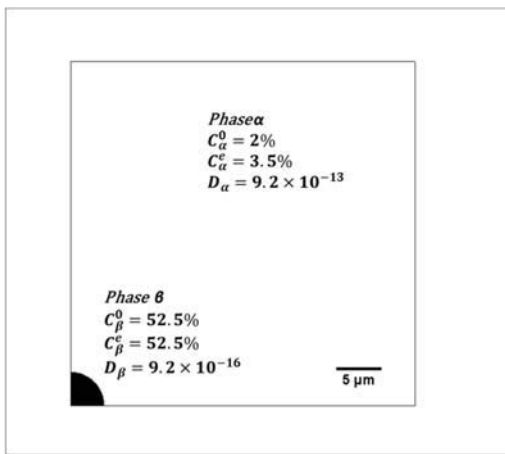
The 2D validation of the model involved comparing the dissolution rate of a circular precipitate in a uniform matrix with the approximate solution for smaller times from [14]. A grid size of  $10^{-7}$  m is used. The analytical and numerical solution for a binary system is shown in Figure 2. The numerical solution differs from the analytical solution by a maximum of 0.2 microns at 10s.

The nucleation-growth and coarsening model was validated by replicating the published results in reference [8].

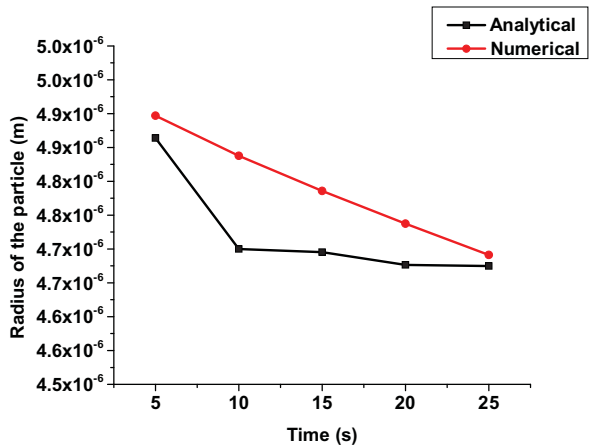


(b)

Figure 1: (a) Initial (5% for  $\alpha$  and 45% for  $\beta$ ); final concentrations (3.5% for  $\alpha$  and 52.5% for  $\beta$ ) and diffusion coefficients ( $4 \times 10^{-14}$   $m^2/s$  for both the phases) for the 2 phase 1D binary model validation experiment. (b) Grid dependent solutions for the binary model and its comparison with the analytical solution.



(a)



(b)

Figure 2: (a) Initial (2% for  $\alpha$  and 52.5% for  $\beta$ ); final concentrations (3.5% for  $\alpha$  and 52.5% for  $\beta$ ) and diffusion coefficients ( $9.2 \times 10^{-13}$   $m^2/s$  and  $9.2 \times 10^{-16}$   $m^2/s$  for  $\alpha$  and  $\beta$  respectively) for the 2 phase 2D binary model validation experiment. (b) The analytical and numerical solutions for a grid size of  $10^{-7}$  m.

## Experiments

### Casting

The Al-0.8Si-1.4Mg alloy was solidified in a cast iron cylindrical mold of 2.5 cm diameter and 15 cm length. Aluminum shot and silicon lumps were melted at 1023 K for the process. Magnesium pieces were added to the melt and the melt was stirred with a graphite rod before pouring. The mold was preheated before pouring. The molten metal and the mold were allowed to cool in air.

The as-cast microstructure consists of non-equilibrium eutectic structure with globules or parallel lamellae of  $Mg_2Si$  particles in  $\alpha$  matrix as seen in Figure 3.

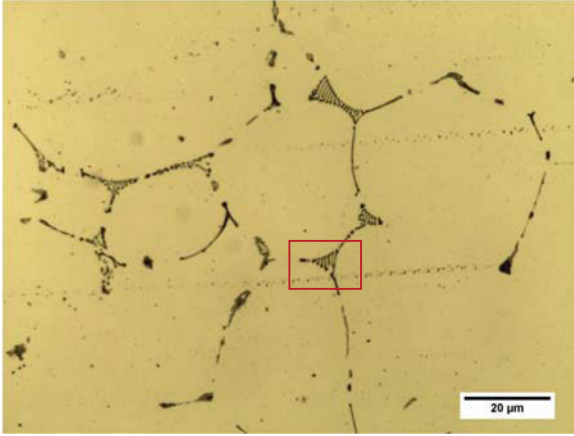


Figure 3: Optical micrograph of the as-cast microstructure. The inset showing the initial condition for the 2-D model

### Phase Characterization

Scanning electron Microscopy images of the as-cast and the homogenized samples were taken using the FEI XL40 SEM

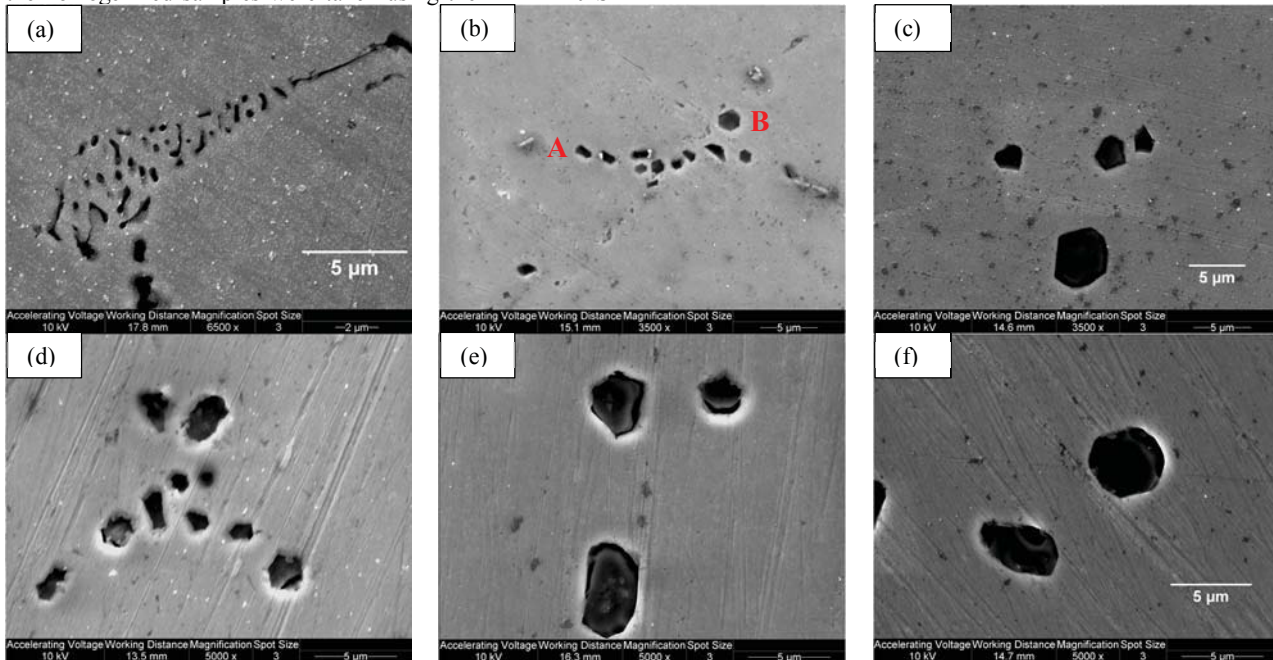


Figure 5: SE images showing the shape and size of the precipitates (a) as-cast and after holding times of (b) 0.5 hr; (c) 1 hr; (d) 2 hrs; (e) 4 hrs and (f) 8 hrs at 823 K.

by FEI. Energy Dispersive X-Ray Spectroscopy using a EDAX Microanalysis setup was done on the as-cast samples to determine the phases present in the as-cast microstructure. The average eutectic composition was found to be 6.9% Mg and 11.3% Si by weight which is close to having 15%  $Mg_2Si$  phase in the eutectic with some excess of Si and some amount of dissolved Al. The volume fraction of the precipitates at any stage was determined from the optical micrographs using ImageJ. The as-cast microstructure consisted of a eutectic volume fraction of 5.2%.

### Homogenization

A temperature of 823 K was chosen for the homogenization temperature for the as-cast alloy as calculated from Thermo-Calc. The samples were homogenized for different holding times of 0.5, 1, 2, 4 and 8 hours in a box furnace. A K-type thermocouple was attached to the sample to monitor the

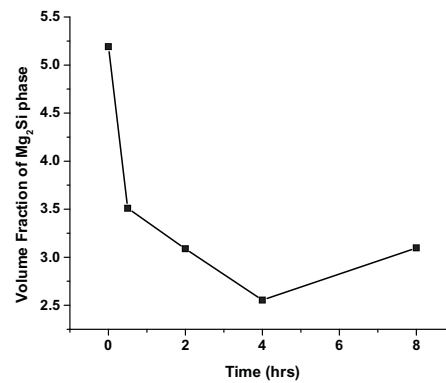


Figure 4: The measured volume fraction of  $Mg_2Si$  phase at different holding times during homogenization at 550°C.

temperature. The volume fraction of the  $Mg_2Si$  phase was determined for a range of holding times (Figure 4). A detailed study of the effect of cooling rate after homogenization is included in a companion paper[15].

During homogenization of the as-cast samples, the eutectic breaks down into particles of  $Mg_2Si$  with well defined facets. The particles are either rectangular (Precipitate A in Figure 5(b)) or hexagonal (Precipitate B in Figure 5(b)) pertaining to the cubic or hexagonal crystal structure of  $\beta$  and  $\beta'$   $Mg_2Si$  phases respectively [16]. On further heating the samples, the precipitates gradually become spheroidised. The EDS measurements of the precipitates were made and the precipitates were found to be deficient in Mg compared to the stoichiometric ratio of 2:1, as has been reported in [3].

Figure 4 suggests an exponential decay of the volume fraction of the precipitates with time until it tends to get flattened at longer time durations. After 8hrs of holding time the particles get coarsened. Four hours seems to be an appropriate holding time for the alloy for homogenization. The length scales of the precipitates at different holding times and their shapes are shown in Figure 5.

## Results and Discussion

### Dissolution Kinetics

A microstructure similar to that of the inset in Figure 3 is used for the initial condition of simulations of the homogenization process. The composition of the alloy is 1% Si and 1.6% Mg. The homogenization process is simulated at 4 different temperatures: 760 K, 780 K, 800 K and 820 K. The

equilibrium volume fractions of  $Mg_2Si$  phase at these temperatures are 1.54%, 1.32%, 0.77% and 0.77% respectively. The equilibrium volume fraction information is from Thermo-Calc. The average eutectic composition of 6.4% Si and 10.6% Mg

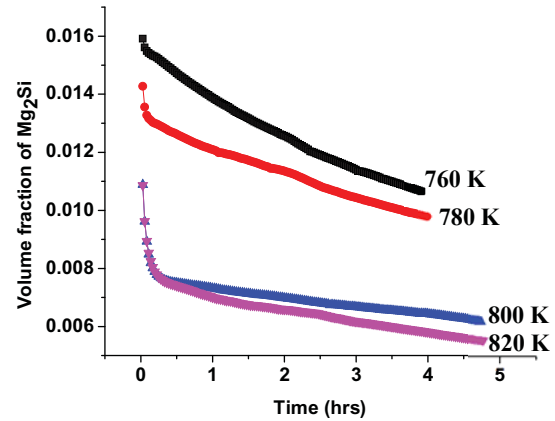


Figure 6: Simulated dissolution kinetics of the precipitates at different temperatures from the 2-D CA-FV model.

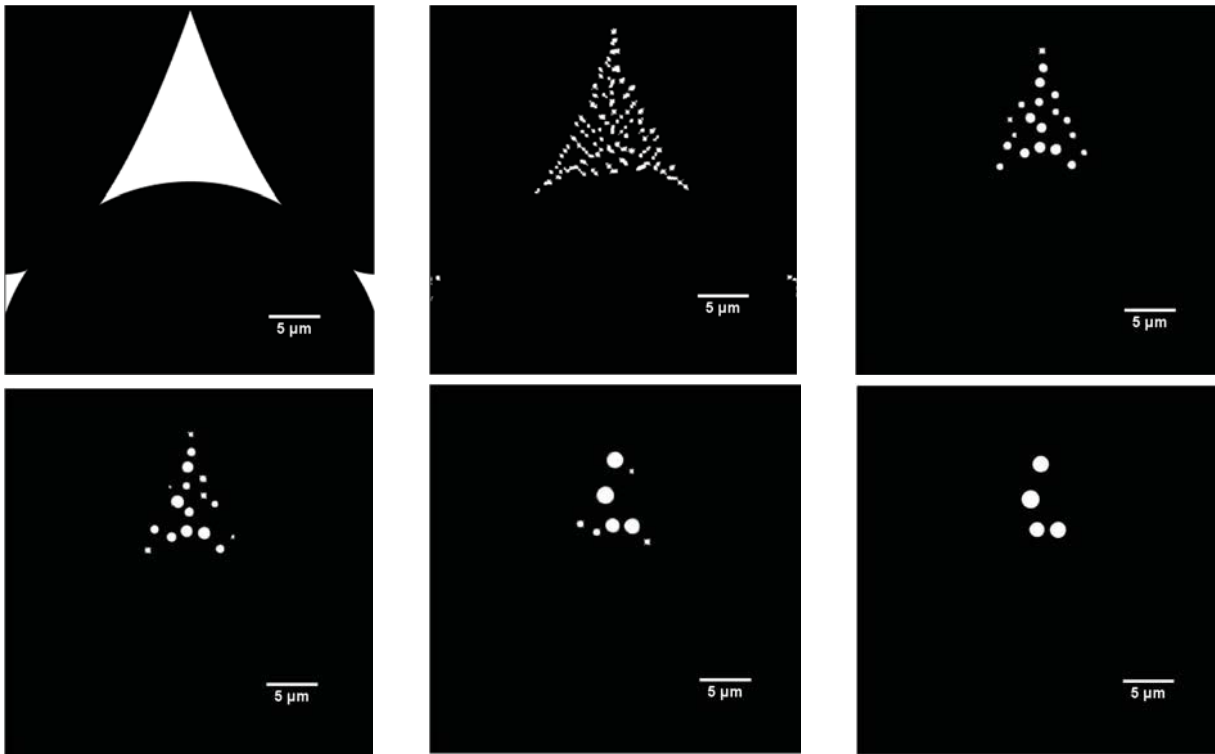


Figure 7: (a) Initial microstructure; and microstructures after (b) 10s; (c) 0.5 hrs; (d) 1 hr; (e) 2 hr and (f) 3 hr of homogenization at 823 K.

is used. The region with the eutectic composition almost instantaneously (within the first couple of seconds) breaks into globular  $Mg_2Si$  particles which form 15% of the eutectic volume fraction. The elongated precipitates are spheroidised with time. It should be noted that the current model does not simulate faceting of the particles.

The microsegregation created during solidification is substantially removed within the first 10-15 minutes of homogenization. The  $Mg_2Si$  volume fraction decays exponentially with time (Figure 6). The general trend matches with the trend found experimentally and by Vermolen et al.[4]. The decay is slower for lower temperatures as compared to the higher temperatures. The curve for 820 K seems to flatten at 4.5 hrs, which seems to be the average time required for optimum homogenization. This time matches with the optimum time (when the microsegregation is gone; the eutectic breaks down into smaller precipitates which are spheroidized) of 4 hours found experimentally as mentioned earlier.

The growth or dissolution of individual precipitates is governed by both the phase diagram information of equilibrium concentrations and the interface curvature. After the precipitate and matrix reach equilibrium concentrations for a given temperature, the growth or dissolution of the precipitates is governed entirely by the curvature effects and larger precipitates grow at the cost of the smaller ones. The overall volume fraction decreases in the process indicating dissolution is faster than growth. It should be kept in mind that the model cannot resolve precipitates smaller than the grid size of the domain which can accelerate the dissolution rate of a precipitate after reaching a minimum radius. The volume fraction decreases beyond the equilibrium volume fraction due to curvature. The length scale of the precipitates match the experimental length scales as seen in Figures 5 and 7.

### Effect of Cooling rate

The effect of cooling rate after homogenization is studied using the 1D finite difference model described in [8] for a Al-Si-Mg alloy containing 0.63% Mg which matches the general range for 6xxx series Al alloys. Three different cooling rates of 1000 K/hr, 500 K/hr and 250 K/hr are chosen for study which is in the range of the industrial cooling rate of 300-500 K/hr [2]. The size distribution of the precipitates found by the numerical model, for different cooling rates is given in Figure 8. There is a bimodal distribution of precipitates, one of the sizes being in the nanometer range and the other being in hundreds of nanometer range. The precipitates in the hundreds of nanometer range are visible through the optical microscope as detailed in a companion

paper in this volume [15]. The precipitates in the nanometer range are merely clusters of atoms presence of which can be confirmed through a Transmission Electron Microscope (TEM).

As the temperature decreases, there is no nucleation of precipitates for the first 8, 16 and 32 minutes for 1000, 500 and 250 K/hr cooling rates, respectively, as there is no super-saturation. On further cooling the super-saturation increases, leading to precipitation of  $Mg_2Si$  particles which later grow to the hundreds of nanometer range due to diffusion and availability of Mg and Si concentrations in the matrix. As these precipitates grow, there is an instantaneous decrease in the mean Mg concentration of the matrix which leads to an increase in the free energy for heterogeneous nucleation leading to a decrease in the nucleation rate. But, on cooling further, the equilibrium concentration of the matrix phase decreases drastically increasing the supersaturation many-folds which leads to the precipitation of the clusters in the nanometer range. But these precipitates could not grow as the temperature is too low for significant diffusion. On further cooling the nucleation rate again decreases as the temperature is very low.

The volume fraction of the precipitated  $Mg_2Si$  particles decreases with an increase in cooling rate as seen in Figure 9. The slower the cooling rate allows more time for diffusion and so the volume fraction increases. Same is the case with the mean radius of the particles which decreases as the cooling rate increases. The

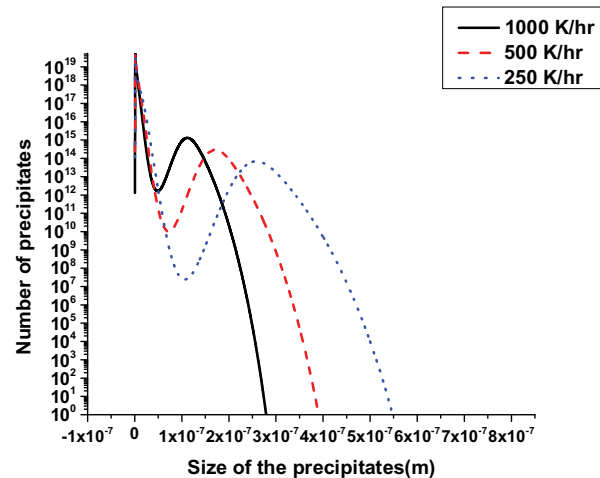


Figure 8: Size distribution of the precipitates for different cooling rates calculated by the 1-D finite difference model.

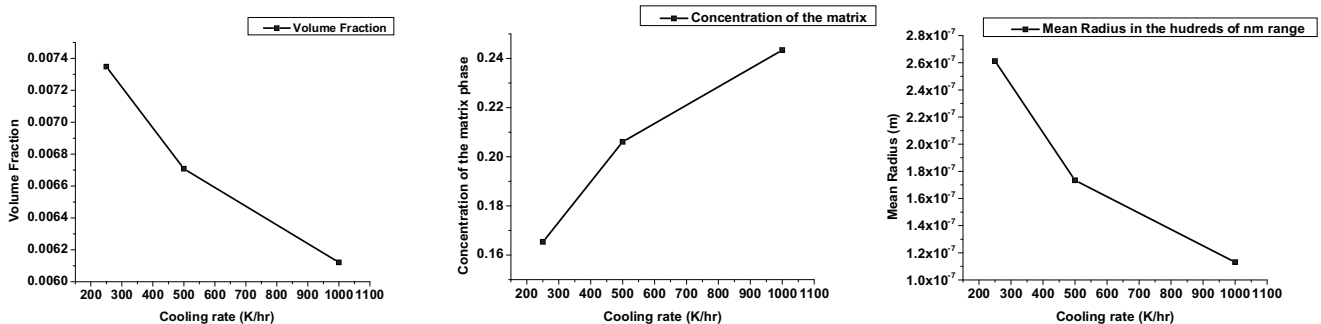


Figure 9: (a) Volume fraction (b) Mg concentration of the matrix and (c) Mean radius in the micrometer range for different cooling rates calculated by the 1-D FD method.

average Mg concentration of the matrix after the precipitation of the Mg<sub>2</sub>Si particles increases with an increase in cooling rate. This is in accordance to the hardness results for samples cooled at different cooling rates in reference [15] which increases as the cooling rate increases due to solid solution strengthening of the Mg present in the matrix.

### Conclusions

The CA-FV model predicts length scales of the Mg<sub>2</sub>Si precipitates which match the experimental length scales. The volume fraction is found to decay exponentially with time. The numerical model is able to predict homogenization times which match experiments. The larger precipitates grow at expense of the smaller ones during homogenization. The volume fraction of the precipitated Mg<sub>2</sub>Si particles and their mean radius decreases with increasing cooling rate after homogenization. The average Mg concentration of the matrix after precipitation is found to be higher for higher cooling rates.

### Acknowledgement

The authors acknowledge financial support from Nanshan America.

### References

- [1] Couper MJ, Cooksey M, Rinderer B, “Effect of Homogenization Temperature and Time on Billet Microstructure and Extruded Properties of Alloy 6061”, Aluminum Cast House Technology VII, TMS(2001), 287-296.
- [2] Rinderer B, “The metallurgy of homogenization”, Mat. Sci. Forum, 693(2011), 264-275.
- [3] Zhu H, Couper MJ, Dahle AK, “Effect of Process Variables on Mg-Si Particles and Extrudability of 6xxx Series Aluminum Extrusions”, JOM, 63(2011), 66-71.
- [4] Vermolen F, Vuik K, Zwaag S, “A mathematical model for the dissolution kinetics of Mg<sub>2</sub>Si-phases in Al-Mg-Si alloys during homogenisation under industrial conditions”, Mat. Sci. and Engg. A254 (1998), 13–32.
- [5] Cai M, Robson J, Lorimer JW, Parson NC, “Simulation of the Casting and Homogenization of two 6xxx series Alloys”, Mat. Sci. Forum, 396-402 (2002), 209-214.
- [6] Haidemenopoulos GN, Kamoutsi H, Zervaki AD, “Simulation of the Transformation of the Iron Intermetallics during Homogenization of 6xxx series extrudable Aluminum alloys”, J of Mat Process Tech, 212 (2012), 2255– 2260.
- [7] Samaras SN, Haidemenopoulos GN, “Modeling of Microsegregation and Homogenization of 6061 extrudable Aluminum alloys”, J of Mat Process Tech, 194 (2007), 63-73.
- [8] Myhr OR, Grong O, Acta Mater., “Modeling a non-isothermal transformations in alloys containing a particle distribution”, 48(2000), 1605-1615.
- [9] Krane MJM, Johnson DR, Raghavan S, “The development of a cellular automaton-finite volume model for dendritic growth “, Applied Mathematical Modeling 33 (2009), 2234–2247.
- [10] Shao R, Trumble K, Krane MJM, “Effects of Geometric Constraints on alloy Solidification in Metal-Matrix Composites”, Modeling of Casting, Welding, and Advanced Solidification Processes – XII, TMS(2009), 495-503.
- [11] Cummins S, Francois M, and Kothe D, “Estimating Curvature from Volume Fractions”, Computers and Structures, 83 (2005), 425.
- [12] Swalin RA, Thermodynamics of Solids, John Wiley and Sons (1962), 147.
- [13] Zhang J, Fan Z, Wang YQ, Zhou BL, “Equilibrium Pseudobinary Al-Mg<sub>2</sub>Si Phase diagram”, Mat. Sci. and Tech, 17(2001), 494-496.
- [14] Whelan MJ, “On Kinetics of Precipitate Dissolution”, Metal Science, 3(1969), 95-97.
- [15] Sun Y, Johnson DR, Trumble K, Priya P, Krane MJM, “Effect of Mg<sub>2</sub>Si Phase on Extrusion of AA 6005 Aluminum Alloy”, Light Metals 2014: Aluminum Processing, TMS(2014).
- [16] Zajac S, Bengtsson B, Johansson A, Gullman L, “Optimisation of Mg<sub>2</sub>Si Phase for Extrudability of AA 6063 and AA 6005 Alloys”, Mat. Sci. Forum, 217-222 (1996), 397-402.
- [17] Morillon TYM, “Predictions of secondary phase dissolution during heat treatment of a Ni-Cr-Mo alloy”, Master’s Thesis, Purdue University, School of Materials Engineering (2004) p30.